Molecular mechanism of honeysuckle + forsythia in treatment of acute lung injury based on network pharmacology

XIN WEN[1], MIN CHENG[1,2], ZHONGXING SONG[1], JINHANG HU[1], XUHU LIANG[2], WUYING LANG[2], MENGQI YANG[1], RUINA ZHOU[1] and YUNJING HAO[3]

[1]Shaanxi University of Chinese Medicine, Co-construction Collaborative Innovation Center for Chinese Medicine Resources Industrialization by Shaanxi and Education Ministry, State Key Laboratory of Research and Development of Characteristic Qin Medicine Resources (Cultivation), Xianyang, Shaanxi 712046; [2]Shangluo University, College of Biomedical and Food Engineering, Shangluo, Shaanxi 726000; [3]Northwest University, College of Life Sciences, Xian, Shaanxi 710075, P.R. China

Received December 30, 2022; Accepted August 8, 2023

DOI: 10.3892/br.2024.1720

Abstract. The pathogenesis of acute lung injury (ALI) is complex and it is a common critical illness in clinical practice, seriously threatening the lives of critically ill patients, for which no specific molecular marker exists and there is a lack of effective methods for the treatment of ALI. The present study aimed to investigate the mechanism of action of honeysuckle and forsythia in treatment of acute lung injury (ALI) based on network pharmacology and *in vitro* modeling. The active ingredients and targets of honeysuckle and forsythia were predicted using traditional Chinese medicine systems pharmacology, PubChem and Swiss Target Prediction databases, and the Cytoscape 3.7.2 software was used to construct a drug-component-potential target network. The potential targets were imported into the Search tool for recurring instances of neighboring genes) database to obtain protein-protein interactions and subjected to Gene Ontology and Kyoto Encyclopedia of Genes and Targets analysis using Database for Annotation, Visualization, and Integrated Discovery. AutoDock Vina 1.1.2 software was used for docking between key active ingredients and the target proteins to analyze the binding ability of the active ingredients to the primary targets in honeysuckle and forsythia. A total of 64 male BALB/c mice were randomly divided into control, model, positive drug (Lianhua-Qingwen capsule), honeysuckle, forsythia, honeysuckle + forsythia high-, medium- and low-dose groups. Lipopolysaccharide (LPS) was used to induced an ALI model. The lung tissues of the mice were stained with hematoxylin-eosin and the serum levels of malondialdehyde (MDA) and the activities of superoxide dismutase (SOD) and glutathione peroxidase (GSH-Px) were measured 4 h after the LPS administration. Reverse transcription-quantitative PCR and western blotting were used to detect NF-κB mRNA and protein expression, respectively. Active ingredients of honeysuckle and forsythia acted on 265 common targets in ALI, which regulated NF-κB, tumor necrosis factor-α (TNF-α) and PI3K-AKT signaling pathway, HIF-1 signalling pathway to slow the inflammatory response in treatment of ALI. In the positive drug group, honeysuckle, forsythia group, honeysuckle + forsythia high-, medium- and low-dose groups, lung tissue damage were significantly decrease compared with the model group, and inflammatory cell infiltration was reduced. Compared with the model group, honeysuckle + forsythia groups experienced decreased damage caused by the LPS and inflammation in the lung tissues and significantly decreased TNF-α and NF-κB and MDA concentration and significantly increased the SOD and GSH-Px activities. The mechanism of the effect of honeysuckle and forsythia on ALI may be mediated by inhibition of TNF-α and NF-κB expression and the activation of antioxidant mechanisms to decrease production of pro-inflammatory cytokines in lung tissue, thus treating ALI.

Correspondence to: Professor Min Cheng, Shangluo University, College of Biomedical and Food Engineering, 10 Beixin Street, Shangluo, Shaanxi 726000, P.R. China
E-mail: chengmin_prof@126.com

Key words: honeysuckle, forsythia, acute lung injury, network pharmacology, molecular docking, TNF-α, NF-κB

Introduction

The pathogenesis of acute lung injury (ALI) is complex (1). It may be triggered by factors such as inflammation, infection and chemical injury, but its pathological mechanism has not been fully elucidated yet. Studies on inflammatory mechanisms have shown that neutrophils serve a crucial role in both pro-inflammatory and anti-inflammatory mechanisms (2,3). Their mechanism may be related to the production of chemokines by macrophages. Chemokines stimulate release of cytokines from macrophages, destroying normal tissue and organ structures and causing dysfunction, which leads to development of ALI (4). ALI is a common critical disease in clinical practice with a high mortality rate (5), mortality rates of up to 60 per cent have been reported for some patients and about 40 per cent overall (6). It threatens survival and quality of life of critically ill patients (6). Moreover, there are no specific molecular markers nor effective methods of treating ALI, so it is urgent to find effective and affordable drugs with few toxic side effects.

The potential of several herbs for the treatment of ALI has been studied by Ma (7) and Xue (8). Honeysuckle is a traditional Chinese medicine (TCM) with a sweet and cold taste. This is the first flower of a dried flower bud and is composed mainly of luteolin and chlorogenic and isochlorogenic acid. Classified as a member of the heart, lung, and stomach meridians in TCM, it disperses wind-heat, clears heat (and detoxifies the body of fever and internal and external carbuncles. It also has antiviral, anti-inflammatory, antioxidant, antipyretic and antibacterial effects (9,10). Forsythia is the dried fruit of the Forsythia plant from the family *Lignanaceae*. It is bitter and slightly cold. It belongs to the heart, lung, and small intestine meridians. It is called the 'medicine for sores' because it is often used in TCM to treat wind-heat, warm diseases, sores, scrofula and astringent pains (11). Pharmacological studies (12,13) have shown that it has broad-spectrum antibacterial, anti-inflammatory, antipyretic, hypotensive, antioxidant and anti-aging effects.

Honeysuckle and forsythia are the primary forms of medication used in TCM. TCM has made progress in the treatment of ALI (14,15), as a variety of herbs used alone or in compounds and active ingredients have shown good therapeutic effects on animal models of ALI. Honeysuckle and forsythia are commonly used as antipyretic drugs (8,9,16). Yinqiao Powder (16,17), which appeared in Wu Jutong's treatise (18,19) on differentiation of febrile diseases, meanwhile, honeysuckle and forsythia are the most classic and commonly used pair of herbs in the formula. Honeysuckle not only clears away the heat in the qi division, but also can detoxify the blood; forsythia is good at promoting blood circulation throughout the body and nourishing the internal organs and tissues. Honeysuckle and forsythia are used in the clinic to improve heat-clearing and detoxification and to disperse wind-heat and also can be used in exopathogenic heat, relieving symptoms, releasing heat and detoxification (20,21). Yinqiao medicine pair is often used in TCM in the form of Yinqiao capsule (22), Qingre jiedu and Shuanghuanglian oral liquid (23,24) and Yinqiao Jiedu tablet (25). Yinqiao medicine enhances the single drug heat-clearing and detoxification, evacuation of wind-heat effect. The present used network pharmacology (26) and molecular docking to construct a drug-target and pathway network of honeysuckle and forsythia for treatment of ALI, and explored the mechanism of action of honeysuckle and forsythia using intraperitoneal lipopolysaccharide (LPS)-induced mouse model of ALI.

Materials and methods

Experimental animals. A total of 64 specific-pathogen-free male BALB/C mice (weight, 18-22 g; 6-8 weeks) were purchased from the Animal Experiment Center of Xi'an Jiaotong University (xian, China), with Certificate of Compliance No. SCXK (Shaanxi) 2008-001. All experimental procedures and protocols were reviewed and approved by the Animal Ethics Committee of Xi'an Jiaotong University and the Animal Ethics Committee of Shaanxi University of Traditional Chinese Medicine. The experiments reported were conducted according to the Guide for the Care and Use of Laboratory Animals (27). The animals were given 1 week to adapt to the experimental conditions before subsequent experiments. They received continuous drug treatment for 7 days. On the 8th day, the mice were injected with LPS on day 8 to establish a model of acute lung injury). The entire experiment lasted 15 days. Pentobarbital sodium anesthesia was administered to all animals and following obtaining lung tissue as well as blood, euthanasia was performed by cervical dislocation. Cessation of breathing and heartbeat was considered to indicate death. The animal room was equipped with 24-h surveillance to monitor the health of the animals. Eating and drinking, urination and defecation and behavior were monitored three times/day. The animals were housed individually in separate cages at 22±1˚C and the humidity was 55±5%. The animals received a 12/12-h light-dark cycle and sterile food and water *ad libitum*. Measures were taken to minimize pain and distress experienced by the animals.

Drugs and reagents. The reagents were as follows: Honeysuckle and forsythia (both Shaanxi Kangcheng Pharmaceutical Co., Ltd.), positive control (Lianhua-Qingwen) (Shijiazhuang Yiling Pharmaceutical Co., Ltd.), LPS (Shanghai Maclean Biochemical Technology Co., Ltd.), malondialdehyde (MDA; cat. No. CB10205), superoxide dismutase (SOD; cat. No. CB10221) and glutathione peroxidase (GSH-Px) kits (cat. No. CB10326) (Nanjing Jiancheng Biological Engineering Co., Ltd.), RNA extraction kit (Shanghai Hendol Biotechnology Co., Ltd.; cat. no. ML12489), NF-κb (1:2,000, cat. no. ab32536, Abcam Co., Ltd.), TNF-α (1:1,000, cat. no. ab183218, Abcam Co., Ltd.) and GAPDH antibody ((1:5,000, cat. no. 60004-1-Ig, ProteinTech Co., Ltd.) and reverse transcription kit (cat. no. #K1622, Thermo Co., Ltd.).

Screening of active ingredients of honeysuckle and forsythia. TCM Systems Pharmacology Database and Analysis Platform (TCMSP) database (tcmspw.com/tcmsp.php) and Encyclopedia of TCM (ETCM; tcmip.cn/ETCM/index.php/Home/Index/) were used to screen the active ingredient targets of honeysuckle and forsythia based on oral bioavailability (OB) ≥30% and drug-like (DL) properties ≥0.18 (28,29). SwissTargetPredicition database (swisstargetprediction.ch/) was used to add the vacant component targets and the UniProt database (uniprot.org/) was entered, limiting the species to human and correcting the name of component targets to obtain the UniProt number.

Honeysuckle and forsythia active ingredient target proteins and ALI target gene collection. PubChem database(https://pubchem.ncbi.nlm.nih.gov) (30) was used to identify honeysuckle and forsythia target proteins. The active ingredients were filtered, relevant target protein names were exported to Microsoft Excel 2010 software (Microsoft Ltd.) and duplicate genes were removed after honeysuckle and forsythia active ingredient-associated target proteins were obtained. In the GeneCards database (31), the keyword 'acute lung injury' was searched to identify target genes associated with ALI. Using the drug and ALI targets, Venn diagrams were constructed with Venny 2.1 software (bioinfogp.cnb.csic.es/tools/venny/index.html) to map the intersecting targets.

Construction of protein-protein interaction (PPI) networks. To understand the mechanism of the drug targets and the disease targets at the protein level, intersecting genes were imported into Search tool for recurring instances of neighboring genes)version 10.5 (string-db.org) to obtain the PPI, after which Cytoscape 3.7.2 software (cytoscape.org/) (32)

was used for network visualization, the CytoNCA 2.1.6 plug-in (https://apps.cytoscape.org/apps/cytonca) (33) was used for network topology analysis and MCODE 2.0.3 (apps.cytoscape.org/apps/mcode) (32) clustering was used for common targets.

Gene Ontology (GO) functional and Kyoto Encyclopedia of Genes and Targets (KEGG) pathway enrichment analysis. The gene symbols of potential targets were recorded using the Database for Annotation of Biological Information (DAVID, version 6.8, david.ncifcrf.gov/summary.jsp) and 'OFFICIAL_GENE_SYMBOL' was selected as the Identifier; 'Homo sapiens,' as the species and 'Gene List,' as the list type. GO functional (metascape.org/gp/index.html#/main/step1) and KEGG (https://www.kegg.jp/) pathway enrichment analysis was performed using P<0.05 and were plotted as bubbles using Bioinformatics Analysis Platform (bioinformatics.com.cn/).

Network construction. Cytoscape 3.7.2 was used to construct the active ingredient-target network of honeysuckle and forsythia, in which each node represented the active ingredient and the key target gene. The edges were used to connect the active ingredient and the key target gene and the nodes connected to the network were expressed in degrees.

Molecular docking. Molecular docking analysis was used to calculate the affinity of key hubs in the network. The components of the gene network wherein most of the targets and proteins had a high degree of nodes were selected for molecular docking. The three-dimensional (3D) structure of the ligand was downloaded from the PubChem database (https://pubchem.ncbi.nlm.nih.gov). The 3D structure of the receptor was obtained using the Research Collaboratory for Structural Bioinformatics database (rcsb.org/). The ligands and receptors were repaired using the MGITOOLS 1.5.6 software (ccsb.scripps.edu/mgltools/) and saved as PDBQT files. AutoDock Vina 1.1.2 software (vina.scripps.edu/) was used to test the affinity of the docking between the key active ingredient and target protein. The active center coordinates of the key target and binding energy of the docking were obtained. The final graphical visualization of the molecular docking data was performed with the Discovery Studio 2016 software (http://www.discoverystudio.net/).

Preparation of honeysuckle-forsythia extract. According to the human-mouse drug dose conversion relationship table (34), the daily dose of honeysuckle and forsythia for adults is 15 g and the converted dose for mice (mean weight, 20 g is (15x0.0026) 0.039 g. In this experiment, the dried herbs of honeysuckle and forsythia were crushed with a pulverizer, mixed with distilled water and extracted by heating to 80˚C and reflux for 4 h. The extract was filtered and the residue was extracted again under the same conditions. Then, filtrates were combined by mixing the extracts of honeysuckle and forsythia in equal proportions (0.1950 g/ml honeysuckle +forsythia medium group; 0.0975 g/ml is honeysuckle +forsythia low group; 0.3900 g/ml is honeysuckle +forsythia high group)), after which they were concentrated at -20˚C for 1 week to the manuscript) under reduced pressure and stored at -20˚C for 1 week.

Model grouping. BALB/C mice were randomly divided into normal control, model group, positive drug (Lianhua-Qingwen), honeysuckle, forsythia and honeysuckle + forsythia (H + F) high-, medium- and low-dose groups (n=8/group). The honeysuckle group was gavaged with 0.195 g/ml honeysuckle extract once/day for 7 d; the forsythia group was gavaged with 0.195 g/ml forsythia extract once a day for 7 d; control and the model group were gavaged with 0.195 g/ml physiological saline once/day for 7 d. Drugs were administered as follows: Positive drug, 0.1950 g/ml Lianhua-Qingwen continuously once/day; H + F high-, 0.3900 g/ml H + F extract twice daily (morning and evening) continuously; H + F medium-, 0.1950 g/ml H + F extract daily and H + F low-dose, 0.09750 g/ml H + F extract daily continuously. On the eighth day, all groups except normal control group were injected with LPS to induce an acute pneumonia model, as previously described (35). The modeling was successful when destruction of alveolar structure, thickening of alveolar septa and infiltration of the inflammatory cells were observed in lung tissue following hematoxylin-eosin stain) staining. After 4 h, other experiments were performed.

Lung histopathology. Lung tissue was taken from the mice following euthanasia and fixed in 10% neutral formalin solution at 4˚C for 24-48 h, followed by washing with distilled water to rinse the slices), dehydration, paraffin embedding, sectioning (5 μm thick slices) and HE staining (10 min, room temperature). The lung tissue morphology and histopathology were observed under a light microscope (magnification, 200X) with a neutral resin seal.

Lung wet/dry (W/D) weight ratio. Following blood collection 1.0 to 1.5 ml of whole blood can be taken from each mouse, the lung tissue was removed by opening the chest cavity and removing the esophagus and trachea and the wet weight of the tissues was measured. The lungs were placed in an oven at 60˚C for 72 h, after which their dry weight was measured and W/D ratio was calculated as follows: (Wet weight/dry weight) x100%.

MDA concentration and SOD and GSH-Px activity of the lung tissue. Blood samples were collected and centrifuged at 1,3693-1,7894 g at 4˚C for 10 min, supernatants were collected and the lung tissue MDA concentration and SOD and GSH-Px activity were measured using the aforementioned kits according to the manufacturer's instructions.

RT-quantitative (q)PCR. Total RNA of mouse lung tissue homogenates was extracted via the TRIzol (Thermo Fisher Scientific, Inc.) method, after which 1 μg RNA was reverse-transcribed using the aforementioned kit according to the manufacturer's instructions. Amplification system: SYBRGreen (cat. no. F-415XL; Thermo Co., Ltd.) Mix 10 μl, upstream primer F 0.4 μl, downstream primer R 0.4 μl, ddH2O 7.2 μl, cDNA template 2 μl, total volume 20 μl. Amplification conditions: 94˚C for 10 min, (94˚C for 20 sec, 55˚C for 20 sec, 72˚C for 20 sec) 40 cycles. Data were analyzed using ABI Prism 7500 SDS 2.0.6 software (.thermofisher.com/us/en/home/technical-resources/software-downloads/applied-biosystems-7500-real-time-pcr-system.html) supplied with the instrument. Primer sequences were as follows: NF-κB forward (F), CCAACC TGAAAATCGTGA and reverse (R), 5'-ACATCTGTGGGG GAAAAG-3'; TNF-α F, 5'-TCTACTGAACTTCGGGGT-3' and R, 5'-GAGTGTGAGGGTCTGGGC-3' and GAPDH F,

Table I. Compounds of honeysuckle and forsythia.

A, Honeysuckle

Compound	OB, %	DL
(Trans-trans) farnesol, 3,7,11-trimethyldodeca-2,6,10-trien-1-ol, farnesol	NA	NA
Sitosterol, Î'-sitosterol	NA	NA
Carvacrol	NA	NA
Ethyl palmitate	NA	NA
Stigmasterol	NA	NA
Î'-terpineol	NA	NA
3'-caffeoylquinic acid, 5'-caffeoylquinic acid, chlorogenic acid, heriguard	NA	NA
Alexandrin, daucosterol, caproic acid, eleutheroside A, sitogluside, strumaroside, Î'-sitosterol-Î'-D-glucoside	NA	NA
Hederagenin	NA	NA
Luteolin	NA	NA
Benzyl ethyl alcohol, phenylethanol	NA	NA
Geraniol, sabinene hydrate	NA	NA
Eugenol, guaiacol	NA	NA
Methyl linoleate	NA	NA
(E)-aldosecologanin	NA	NA
Benzyl benzoate	NA	NA
3'-methoxyluteolin, chrysoeriol	NA	NA
6'-O-(7Î'-hydroxyswerosyloxy)loganin	NA	NA
Linalyl oxide	NA	NA
Loganic acid	NA	NA
Loganin	NA	NA
Lonicerin	NA	NA
Macranthoidin A	NA	NA
Macranthoidin B	NA	NA
3'-O-methyl loniflavone	NA	NA
3-methyl-2-(2-pentenyl)-2-cyclopenten-1-one	NA	NA
L-phenylalaninosecologanin	NA	NA
Mandenol	42.00	0.19
Ethyl linolenate	46.10	0.20
Eriodyctiol (flavanone)	41.35	0.24
4,5'-retro-β, β-carotene-3,3'-dione, 4',5'-didehydro-	31.22	0.55
5-hydroxy-7-methoxy-2-(3,4,5-trimethoxyphenyl) chromone	51.96	0.41
Stigmasterol	43.83	0.76

B, Forsythia

Compound	OB, %	DL
Dimethylesculetin, scoparone	NA	NA
Î'-Terpineol	NA	NA
Oleanolic acid	NA	NA
D-camphene	NA	NA
D-limonene, limonene, dipentene, Î'-phellandrene	NA	NA
(E)-citral,3,7-dimethylocta-2,6-dienal, citral-B	NA	NA
Camphor	NA	NA
P-cymol, P-cymene, umbelliferone	NA	NA
Ursolic acid	NA	NA
Acteoside, verbascoside	NA	NA
1-isopropyl-4-methylcyclohexa-1,4-diene, terpinolene, Î'-terpinene	NA	NA
Wogonoside	NA	NA

Table I. Continued.

B, Forsythia

Compound	OB, %	DL
3Î'-acetyl-20,25-epoxydammarane-24Î'-ol	NA	NA
Forsythenside A	NA	NA
Forsythoside C	NA	NA
Isobauerenyl acetate	NA	NA
Lactose	NA	NA
Matairesinoside	NA	NA
Phillygenin	NA	NA
Phillyrin	NA	NA
Rengyolone	NA	NA
Rengyoside B	NA	NA
Safrole	NA	NA
Suspenolic acid	NA	NA
Wogonin	30.68	0.23
(2R,3R,4S)-4-(4-hyd roxy-3-methoxy-phenyl)-7-methoxy-2,3-dimethyl60ol-tetralin-6-ol	66.51	0.39
(3R,4R)-3,4-bis[(3,4-dimethoxyphenyl) methyl] oxolan-2-1	52.30	0.48
Mairin	55.38	0.78
Hyperforin	44.03	0.60
Onjixanthone I	79.16	0.30
β-sitosterol	36.91	0.75
Arctiin	34.45	0.84
Luteolin	36.16	0.25
Bicuculline	69.67	0.88

C, Honeysuckle and forsythia

Compound	OB, %	DL
Linalool	NA	NA
Kaempferol	41.88	0.24
Quercetin	46.43	0.28

NA, not available; OB, oral bioavailability; DL, drug-like.

5'-GGTGAAGGTCGGTGTGAACG-3' and R, 5'-CTCGCT CCTGGAAGATGGTG-3'. Data were normalized to expression of GAPDH RNA as endogenous control and quantified using the $2^{-\Delta\Delta cq}$ method (36) *Western blotting*. Mouse lung tissue was lysed with 1:100 PMSF and the standard curve was plotted and quantified by BCA. Then, 30 μg protein/lane was separated by electrophoresis, transferred to PVDF membranes and blocked with 5% BSA (cat. no. A9647; BIOSHARP Co., Ltd.) at room temperature for 1 h. The primary NF-κB (1:2,000, species: rabbit, 12% Gel), TNF-α (1:1,000, species: rabbit, 15% Gel) and GAPDH antibody (1:5,000, species: mouse, 12% Gel) and Tween-20 (0.05%); company: Amresco; cat: BYL40713, incubated with the membrane overnight at 4˚C. The membrane was washed five times with TBST for 10 min each time, followed by incubation with 1:5,000 secondary antibody for 1 h at 37˚C. The membrane was washed five times with TBST for 10 min each time, after which developed using an ECL kit (Beijing Dingguo Ltd.; cat:ECL-0011) and the bands were analyzed using the Image J 1.8.0 software (National Institutes of Health).

Statistical analysis. The data obtained were analyzed using version 26.0, SPSS (IBM Corp.). Data are expressed as the mean ± standard deviation of 3 independent experiment). One-way ANOVA followed by Dunnett's post hoc test was used for analysis. P<0.05 was considered to indicate a statistically significant difference.

Results

Active ingredient screening and target determination. Using the TCMSP and ETCM databases, 33 chemical components of honeysuckle, 35 chemical components of forsythia and three chemical components of H + F were screened according to OB≥30% and DL≥0.18 (duplicates were removed; Table I).

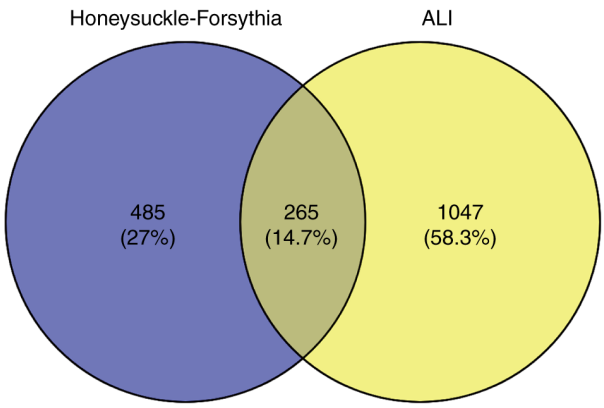

Figure 1. Venn diagram of targets of honeysuckle and forsythia components and ALI. The 485 potential targets of the honeysuckle and forsythia were mapped to the 1,047 targets of ALI. A total of 265 potential targets for Gene Ontology analysis were obtained. ALI, acute lung injury.

Prediction of potential targets. ALI targets were obtained from the GeneCards database, and the Venny 2.1 mapping tool was used to map honeysuckle and forsythia to them (Fig. 1). Honeysuckle and forsythia may act together to treat ALI through multiple potential targets.

PPI network construction. PPI network was obtained by inputting the 265 common targets of honeysuckle and forsythia and ALI into the STRING database and visualizing the network using Cytoscape 3.7.2 (Fig. 2A). The network involved 265 nodes and 5,949 edges. The results of the network topology analysis showed that the mean node degree was 44.9. The key targets GAPDH, albumin (ALB), Akt1, TNF, IL-6 and vascular endothelial growth factor A (VEGFA) were screened based on the node values (Fig. 2B) and were hypothesized to have a key role in the treatment of ALI by honeysuckle and forsythia.

GO enrichment analysis. The 265 intersecting targets were entered into the DAVID database and a total of 3,474 GO enrichment entries were obtained, including 3,078 biological processes, 120 cell components and 276 molecular functions. The top five GO entries in each category were plotted on a bubble diagram (Fig. 3A). The biological processes such as 'cellular response to oxidative stress' and 'transmembrane receptor protein kinase activity', 'protein tyrosine kinase activity', and 'protein serine/threonine kinase activity' all served an important role in the treatment of ALI.

KEGG pathway enrichment analysis. The 183 signaling pathways were screened in KEGG and the top 20 entries were plotted on a bar graph (Fig. 3B). The main pathways associated with ALI were 'lipid and atherosclerosis', 'EGFR tyrosine kinase inhibitor resistance', 'PI3K-Akt signaling pathway', 'HIF-1 signaling pathway', 'TNF signaling pathway' and 'proteoglycans in cancer'.

Component-target-pathway network. Cytoscape was used to construct the component-target-pathway network (Fig. 4). The network had 223 nodes with 57 components, 146 targets, 20 pathways and 892 edges. The number of associations between the nodes was predicted by the degree. Higher degrees indicate more important components/targets.

Molecular docking. Based on primary active components of the component-target-pathway network, the five components of the gene network whose targets and proteins had the most high nodes were selected for molecular docking. Table II shows key targets and the binding energy for docking. Lower free energy for molecular docking represents a higher affinity between receptor and the ligand. The compounds that most strongly bound to each protein were visualized (Fig. 5). The binding energy of each compound was <-6 kcal/mol, which indicated that each compound bound well to each protein, except for loganin, (3R,4R)-3,4-bis [(3,4-dimethoxy phenyl) methyl] oxolan-2-one, TP53 and IL6. Hederagenin had the highest affinity with ALB and AKT1 and luteolin had the highest affinity with TNF, TP53, and IL6. To verify these results, molecular docking analysis was used to calculate the affinity of the key hubs in the network. Hederagenin has high affinity for ALB, AKT1 and Luteolin for TNF, TP53, IL6.

General performance of mice. The mice exhibited no abnormal respiratory sounds, normal diet and water intake and urine and stool output, rapid response to noise. Following intraperitoneal injection of LPS, the mice appeared to be depressed and exhibited scratching, inactivity, huddling and slow responses, as well as trembling, accelerated breathing and heart rate and decreased drinking.

HE staining. Under a light microscope, it was found that the normal group had intact lung tissue structure, clear alveolar cavities and no inflammatory cell infiltration in interstitial (Fig. 6A). In the model group, there was notable alveolar granulocyte aggregation and multiple hemorrhages in the tissue; a number of blood vessels were congested and alveolar walls were thickened (Fig. 6B). In the Lianhua-Qingwen group, there was little granulocyte aggregation, multiple hemorrhages in the tissue but few exfoliated cells in the alveolar cavities; many blood vessels were congested and the local alveolar walls were thickened (Fig. 6C). In the honeysuckle group, there was notable granulocyte aggregation, multiple hemorrhages in the tissue but few exfoliated cells in the alveolar cavities; a small number of the blood vessels were congested, local alveolar walls were thickened and a small amount of powdery protein-like material was exuded (Fig. 6D). In the forsythia group, there was little granulocyte aggregation, bleeding in numerous places, alveolar cavities contained some shedding cells, few blood vessels were congested, alveolar walls were thickened and a small amount of powder-stained protein-like material was exuded (Fig. 6E). In the H + F high-dose group, there was certain granulocyte aggregation, tissues were locally hemorrhagic, alveolar cavities contained a few decidual cells, the local blood vessels were congested and the alveolar walls were notably thickened (Fig. 6F). In the H + F medium-dose group, few granulocytes aggregated, there was bleeding in many places, alveolar cavities contained some shedding cells, the local blood vessels were congested and the alveolar wall was thickened (Fig. 6G). In the H + F low-dose group,

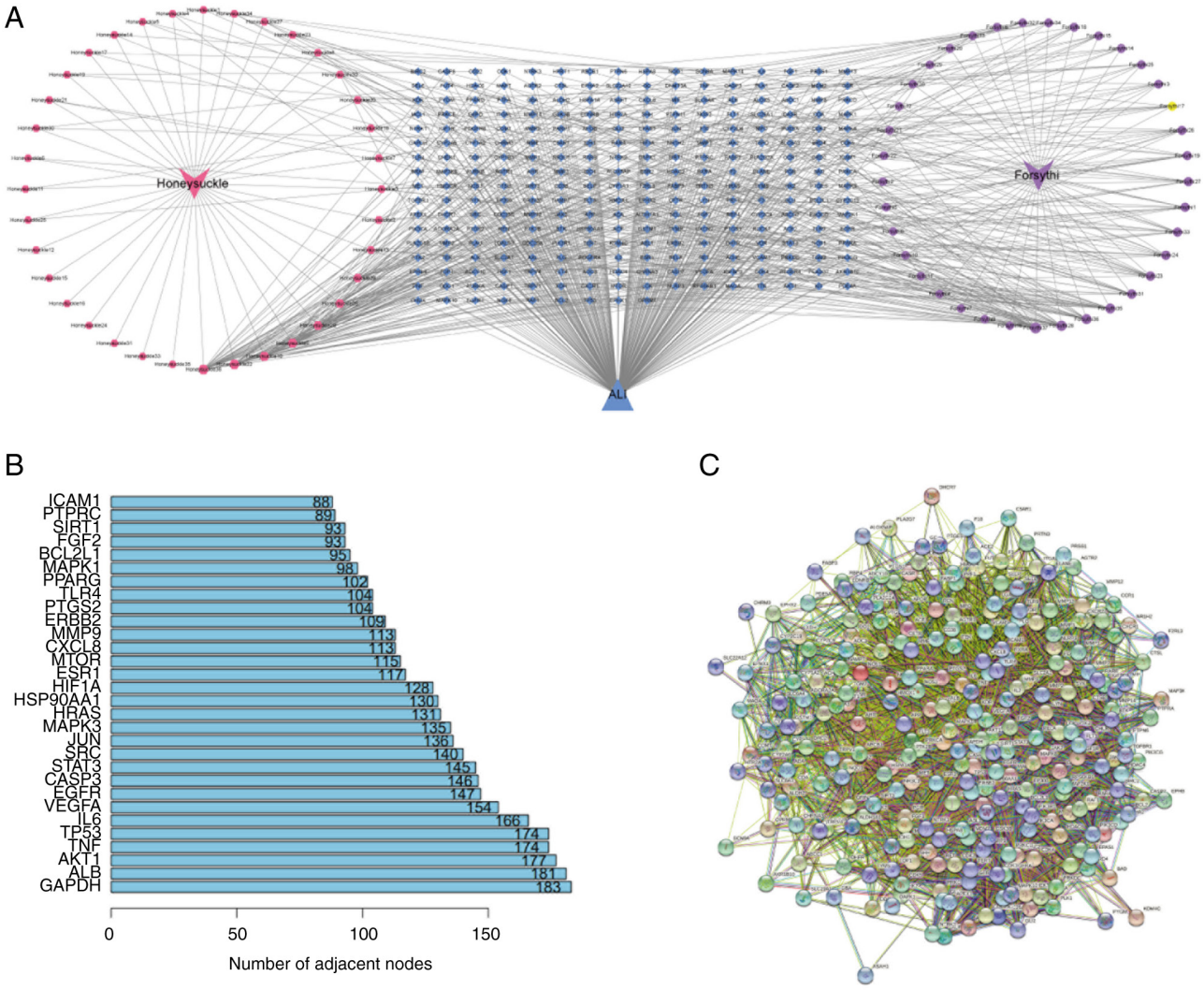

Figure 2. Network construction and topology analysis. (A) Component-disease-target network. (B) Ranking of core targets. (C) Protein-protein interaction network of potential targets of honeysuckle and forsythia in the treatment of ALI. ALI, acute lung injury.

many granulocytes aggregated, there was tissue hemorrhage and partial hemorrhage in the alveolar cavities, local blood vessels were congested and the alveolar walls were thickened (Fig. 6H). The pathological conditions and inflammatory cell infiltration in the H + F groups were notably decreased compared with those in the model group, which indicated that honeysuckle and forsythia improved LPS-induced ALI in mice.

MDA content and SOD and GSH-Px activity in lung tissue. Compared with the normal group, MDA content of the serum of the mice in the model group increased significantly (P<0.01) and SOD and GSH-Px activities significantly decreased (P<0.01 for both; Table III). Compared with the model group, MDA content of the serum of the mice decreased in the Lianhua-Qingwen (P=0.001), honeysuckle (P=0.025), forsythia (P=0.001) and H + F high- (P=0.04), medium- (P=0.022) and low-dose group (P=0.050); the SOD and GSH-Px activity in the serum of mice increased in Lianhua-Qingwen (P=0.010 and 0.017, respectively), honeysuckle (P=0.004 and 0.019, respectively), forsythia (P=0.002 and 0.021, respectively) and H + F high- (P=0.012 and 0.017, respectively), medium- (P=0.015 and 0.021, respectively) and low-dose group (P=0.022 and 0.019, respectively).

W/D ratio. W/D ratios of the left and right lung and total lung tissues of the mice in the model group were significantly higher than those of mice in the blank control group (all P<0.01; Table IV). W/D ratios of total lung tissues of the mice in the model group were significantly higher than those in the Lianhua-Qingwen, honeysuckle, forsythia and H + F high-, medium- and low-dose group.

RT-qPCR. The expression levels of NF-κB and TNF-α in the model group were significantly higher than those in control, Lianhua-Qingwen, honeysuckle, forsythia and H + F high- and medium-dose group. Compared with control, the expression of NF-κB and TNF-α was significantly higher in the model group (Fig. 7).

Western blotting. The expression of NF-κB and TNF-α in the model group were significantly higher than those in control, Lianhua-Qingwen, honeysuckle, forsythia and H + F high- and medium-dose group; Compared with control, the expression

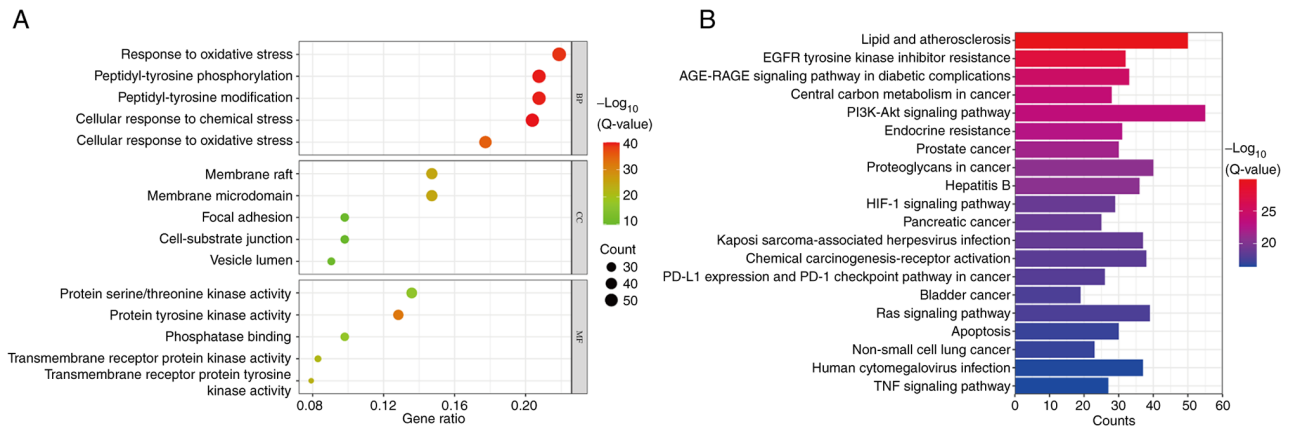

Figure 3. Enrichment analysis of key targets. (A) Gene Ontology functional terms in BP, CC and MF. The top 5 terms in each category are provided. (B) Kyoto Encyclopedia of Genes and Genomes pathway enrichment analysis. The top 20 terms in each category are provided. BP, biological process; CC, cellular component; MF, molecular function.

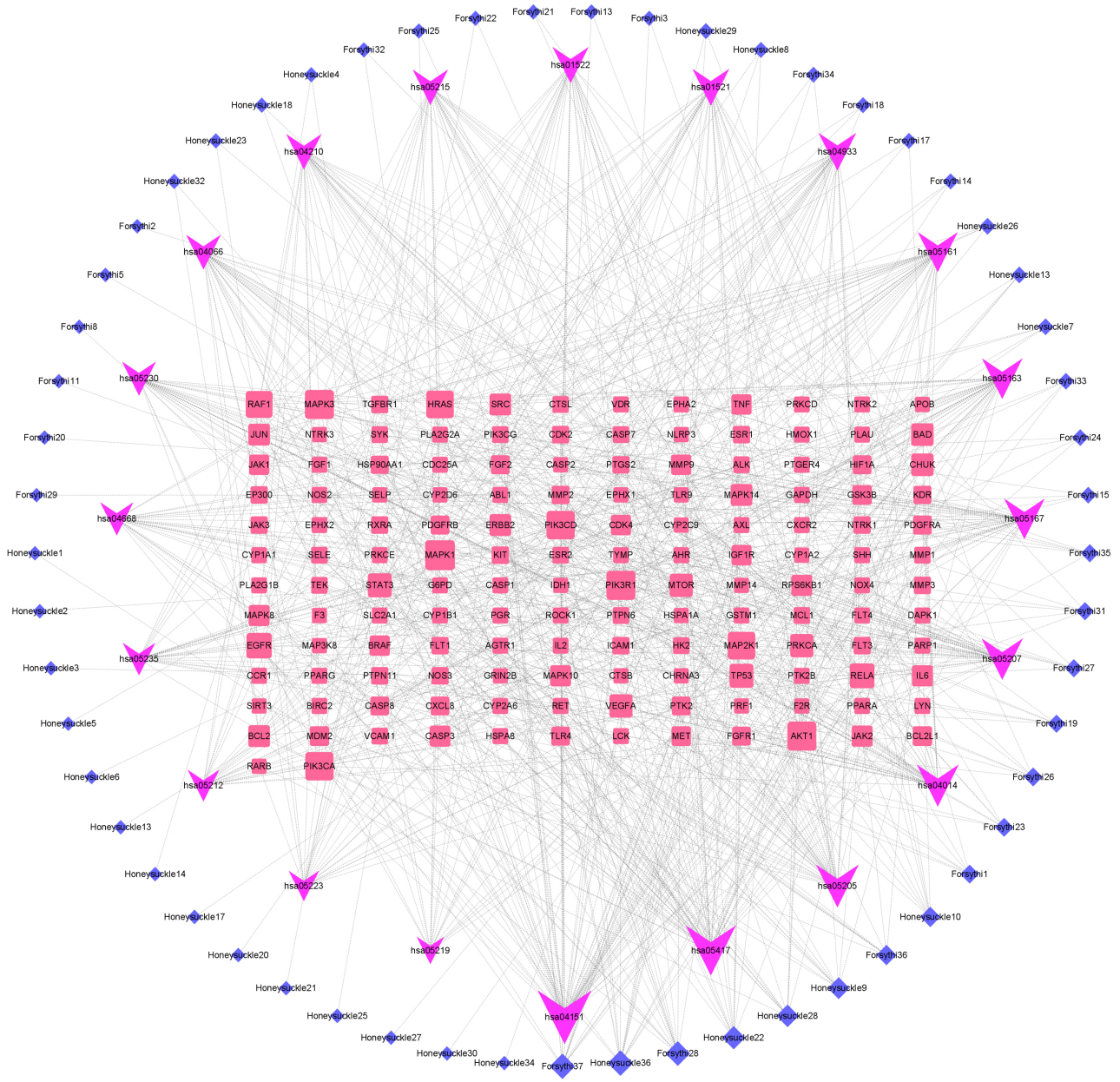

Figure 4. Interaction network of honeysuckle and forsythia and associated pathways. The size and color of nodes represent the degree value. The larger the node, the larger the degree value. Blue diamond, component; pink quadrilateral, target; purple triangle, pathway.

Table II. Binding ability of active components to target proteins.

Active ingredient	Binding energy, kcal/mol				
	ALB	AKT1	TNF	TP53	IL6
Luteolin	-9.0	-9.8	-8.8	-7.2	-6.9
Quercetin	-8.2	-9.2	-7.6	-6.6	-6.7
Hederagenin	-9.6	-10.7	-6.5	-6.3	-6.8
Loganin	-6.9	-6.5	-6.8	-6.6	-6.3
(3R,4R)-3,4-bis[(3,4-dimethoxyphenyl)methyl]oxolan-2-one	-9.0	-9.3	-8.6	-5.7	-5.9

ALB, albumin.

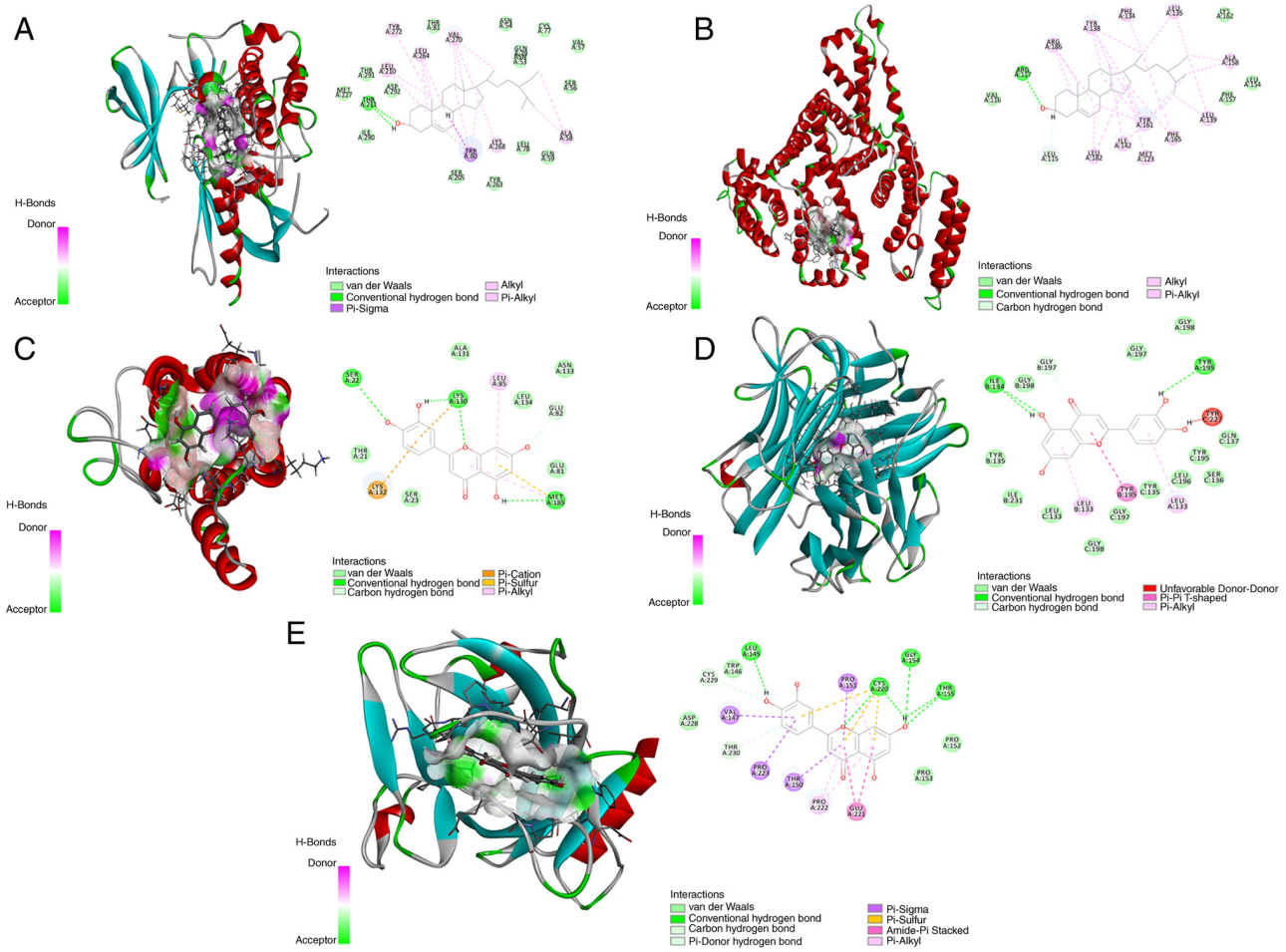

Figure 5. Docking pattern of primary compounds of honeysuckle and forsythia with key target molecules. Molecular docking of hederagenin and (A) AKT1 and (B) albumin and luteolin with (C) IL-6, (D) TNF and (E) TP53.

of NF-κB and TNF-α was significantly higher in the model group (Fig. 8).

Discussion

ALI is a serious lung disease for which there is no effective treatment (37). Thus, there is need to develop ALI treatment strategies. LPS is one of the factors that contribute to ALI by causing fluid to enter lung tissue and increasing the microvascular permeability, which leads to acute tissue inflammation (38). The present study applied network pharmacology techniques and molecular docking to analyze the targets, pathways, and molecular protein aspects of honeysuckle and forsythia drug pair and ALI to explain the disease process and the drug action mechanism (39,40). The establishment of a mouse model of LPS-induced ALI is an effective method as an assessment of lung inflammation and injury (41). Due to pharmacological effects of TCM, researchers have investigated the effects and mechanisms of the active ingredients of TCM on LPS-induced ALI (42,43). Wang *et al* (44) also used a mouse

Table III. MDA content and SOD and GSH-Px activity in lung tissue of mice.

Group	MDA	SOD	GSH-Px
Blank	1.12±0.26	167.78±9.69	73.71±11.55
Model	1.70±0.16[a]	109.53±13.78[a]	36.53±10.58[a]
Positive	1.35±0.06[b]	134.81±14.18[c]	55.02±12.01[c]
H	1.47±0.14[c]	138.67±11.95[b]	54.63±12.03[c]
Forsythia	1.36±0.10[b]	140.67±10.45[b]	54.29±11.48[c]
H + F high-dose	1.40±0.13[b]	134.14±15.83[c]	56.04±11.25[c]
H + F medium-dose	1.47±0.10[c]	133.25±13.29[c]	54.23±10.47[c]
H + F low-dose	1.50±0.16[c]	131.80±12.33[c]	54.62±13.01[c]

P<0.01 vs. [a]blank and [b]model; [c]P<0.05 vs. model. MDA, malondialdehyde; SOD, superoxide dismutase; GSH-Px, glutathione peroxidase; H + F, honeysuckle + forsythia.

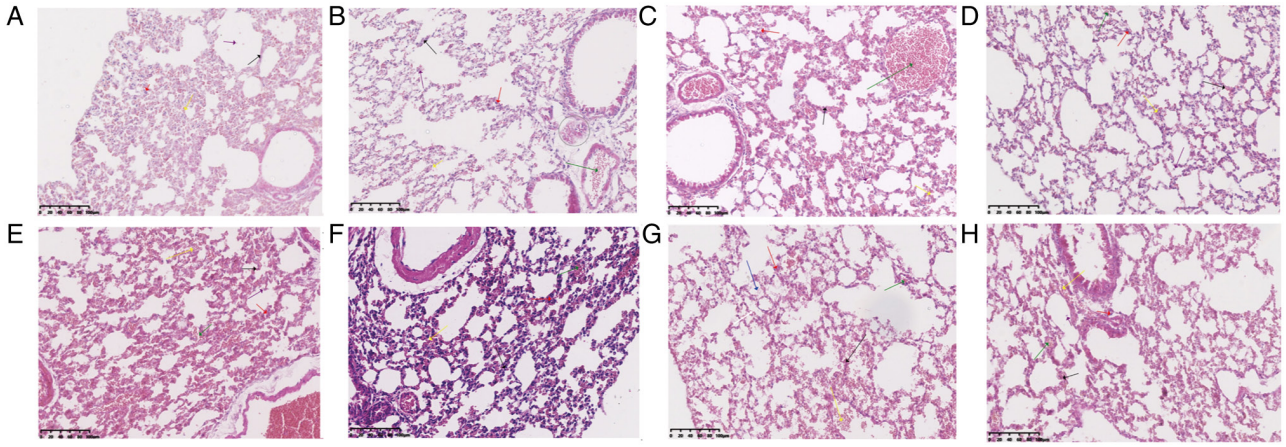

Figure 6. Histopathology of mouse lung by hematoxylin-eosin staining. (A) Blank. (B) Model. (C) Positive. (D) H. (E) F. H + F (F) high-, (G) medium- and (H) low-dose. Red arrow, granulocyte aggregation; yellow arrow, intra-tissue hemorrhage; purple arrow, decidual cells in alveolar lumen; green arrow, intravascular congestion; black arrow, alveolar wall thickening; white arrow, edema; blue arrow, powdered protein-like material. Magnification, x200. H, honeysuckle; F, forsythia.

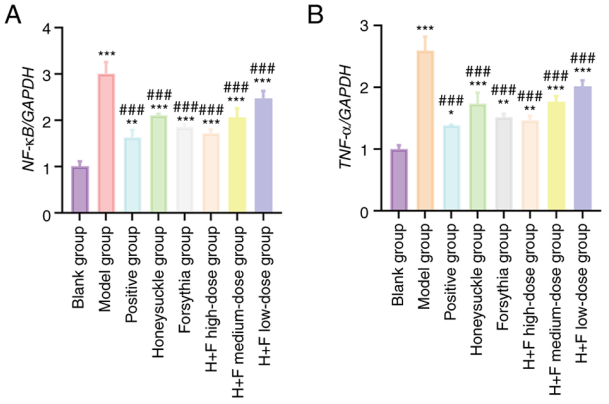

Figure 7. Relative expression of NF-κB and TNF-α in lung tissue of mice. (A) NF-κB. (B) TNF-α. *P<0.05, **P<0.01 and ***P<0.001 vs. blank; ###P<0.001 vs. model. H + F, honeysuckle + forsythia.

model of LPS-induced ALI) model and found that Forsythiae Fructuse exhibited anti-inflammatory effects and protected the epithelial barriers in lungs and colons by regulating PPAR-γ/RXR-α in the treatment of LPS-induced ALI. Therefore, the present study used the intraperitoneal injection of LPS to establish an ALI model in mice and used Lianhua-Qingwen as a positive control to explore the mechanism of action of honeysuckle and forsythia drug pair in the treatment of ALI.

The inflammatory response is an important pathological mechanism of ALI (45). Studies have shown that compound, single-flavor Chinese medicines and active ingredients of Chinese medicines serves an important role in preventing and treating lung injury by inhibiting inflammatory pathways, regulating inflammatory mediators and reducing the release of inflammatory factors (46,47). TCM has potential in the prevention and treatment of ALI. It can significantly improve lung injury by exerting pharmacological effects on signaling pathways and targets (For example, the PI3K/Akt and NF-κB signaling pathways have been studied) of ALI. In the present study, a total of 265 targets were obtained from the component-disease-target network diagram, which suggested that the treatment of ALI with honeysuckle was the result of the combined effect on multiple targets. The GO enrichment analysis showed that the target genes involved in the biological process of ALI treatment were associated with 'cellular response to oxidative stress' and the activation of the transcription factor activity, 'protein

Table IV. Wet/dry weight ratio of left and right lung and total lung tissues of mice.

Group	Left lung	Right lung	Total lung tissue
Blank	0.0542±0.0038	0.0796±0.0045	4.0450±0.3937
Model	0.0923±0.0048[a]	0.1142±0.0395[b]	6.6000±0.5548[a]
Positive	0.0688±0.0068[c]	0.0867±0.0170[c]	4.9475±0.5253[d]
H	0.0659±0.0078[d]	0.0866±0.0248[c]	4.6475±0.5074[d]
Forsythia	0.0648±0.0036[d]	0.0844±0.0202[c]	5.3225±0.9624[c]
H + F high-dose	0.0678±0.0066[c]	0.0872±0.0136[c]	4.7750±0.7760[d]
H + F medium-dose	0.0720±0.0122[c]	0.0884±0.0098[c]	5.2250±1.1453[c]
H + F low-	0.0616±0.0024[d]	0.0831±0.0047[c]	5.2175±1.1521[c]

[a]P<0.01, [b]P<0.05 vs. blank; [c]P<0.05, [d]P <0.01 vs. model. H + F, honeysuckle + forsythia.

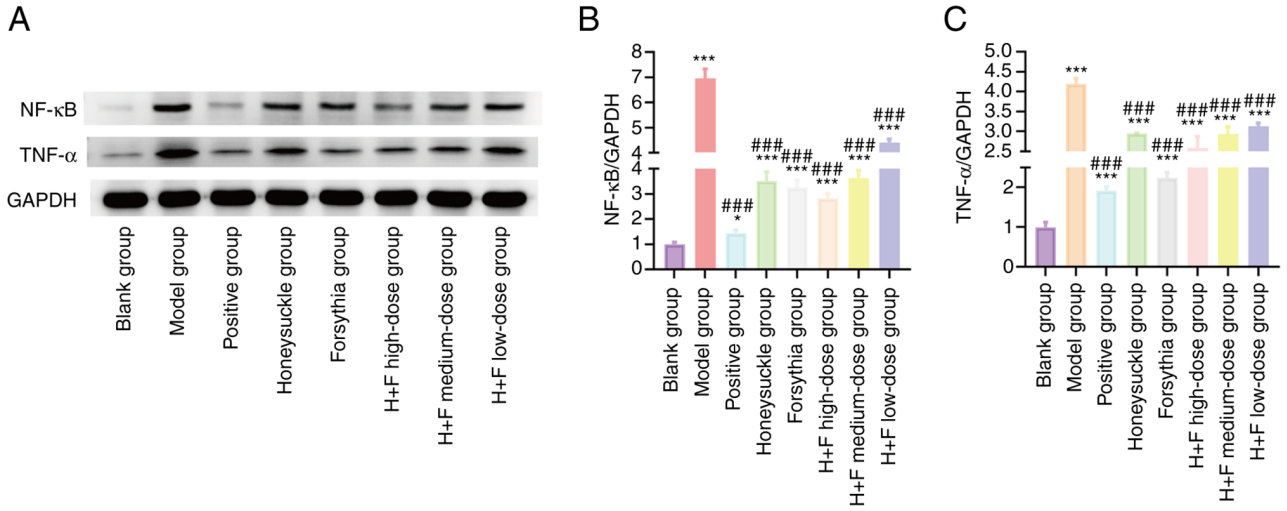

Figure 8. Effect of honeysuckle-forsythia on the expression of pairs of related proteins in mouse lung tissues. (A) Mouse lung tissue levels of NF-κB and TNF-α were detected by western blotting and normalized to GAPDH. Expression of (B) NF-κB and (C) TNF-α in mouse lung tissue. *P<0.05 and ***P<0.001 vs. blank; ###P<0.001 vs. model. H + F, honeysuckle + forsythia.

tyrosine kinase activity' and 'protein serine/threonine kinase activity'. KEGG showed that 183 signaling pathways were screened in the enrichment analysis. The primary pathways associated with ALI included 'lipid and atherosclerosis', 'EGFR tyrosine kinase inhibitor resistance' (48), 'PI3K-AKT signaling pathway' (49,50), 'HIF-1 signaling pathway', 'TNF signaling pathway' (51,52) and 'proteoglycans in cancer'. The results of the HE staining showed that H + F improved the histopathological status of the lungs to different degrees and PCR and western blotting showed that the protein expression of NF-κB (53,54) and TNF-α was significantly decreased in the Lianhua-Qingwen, honeysuckle, forsythia and H + F high- and H+F medium-dose groups. In addition, quercetin (55,56), a common component of honeysuckle and forsythia, and the components of honeysuckle and forsythia with the most targets were selected for molecular docking; hederagenin in honeysuckle was found to have the highest affinity with ALB and AKT1, whereas luteolin in forsythia was found to have the highest affinity with TNF, TP53 and IL6.

The present results further showed that H + F significantly decreased serum MDA and increased SOD activity compared with the model group. Studies have shown that the levels of MDA, a lipid peroxidation reaction end product in the body that causes oxidative damage to lung tissue in pneumonia (57), typically reflect the intensity of lipid peroxidation and cellular damage and the degree of metabolism in the body (58,59). SOD is an antioxidant enzyme that degrades excess oxygen radicals in tissue and its activity reflects the antioxidant capacity and ability to scavenge intracellular oxygen radicals (60). GSH-Px is a key catalytic enzyme for the breakdown of hydrogen peroxide and is widely present in the body (61). SOD and GSH-Px activities can reflect the ability to scavenge oxygen radicals, which plays a role in the oxidative and antioxidant balance of the body (62) and is an important indicator of oxidative stress (63). The present results indicated that levels of oxidative stress in the body were decreased by H + F, which suggested that honeysuckle and forsythia drug pair may decrease lung tissue damage by inhibiting the antioxidant effects.

Moreover, W/D ratio of the lung tissues of the mice in the model group increased significantly compared to control, whereas the W/D ratios of the lung tissues in the honeysuckle,

forsythia, Lianhua-Qingwen and H + F high-, medium- and low-dose groups decreased significantly compared with the model group. Histopathological changes in the lungs of the mice in the model group with ALI caused by LPS were the most obvious, with destruction of alveolar structure, interstitial and alveolar edema and hemorrhage after the LPS injection. These are typical ALI phenomena (64,65). Compared with the model group, mice in the H + F groups showed better lung structural integrity, with relatively thin alveolar walls, some exfoliated cells in the alveolar cavity, less congestion in blood vessels and less inflammatory cell exudation. These results suggest that similar to Lianhua-Qingwen, H + F had a significant effect on lung injury of LPS-induced ALI mice.

In conclusion, the present study applied network pharmacology and *in vivo* validation to analyze the active ingredients, targets and pathways of honeysuckle and forsythia in ALI. Treatment of ALI with H + F may be achieved by combined effects of multiple components, targets and pathways and the active components of honeysuckle and forsythia could significantly decrease the inflammatory response and pulmonary edema in mice with ALI. Its mechanism of action may be associated with inhibition of the expression of TNF-α and NF-κB and the activation of antioxidants, thereby decreasing the ALI caused by LPS in mice. However, this experiment had limitations, such as an incomplete collection of data. Firstly, we used the ETCM database to collect the targets of honeysuckle and forsythia, but the lack of OB (%) and DL values in the ETCM database caused the vacancies in the table we listed; secondly, due to the complexity of the constituents of honeysuckle and forsythia, we only did molecular docking between the top-ranked constituents and the targets, and we will continue to explore the binding of the rest of the constituents and the targets and validate it in the following period; thirdly, in the following period, our group will also continue to pay attention to the study of honeysuckle-forsythia pairs on the cellular level) on whether honeysuckle and forsythia can be safely and effectively applied in the treatment of ALI and multiple mechanisms of their effects, which need to be investigated in greater depth. Nevertheless, the present experiment provided information for clinical application of H + F drug pair in the treatment of ALI.

Limitations

Firstly, we used the ETCM database to collect the targets of honeysuckle and forsythia, but the lack of OB (%) and DL values in the ETCM database caused the vacancies in the table we listed; secondly, due to the complexity of the constituents of honeysuckle and forsythia, we only did molecular docking between the top-ranked constituents and the targets, and we will continue to explore the binding of the rest of the constituents and the targets and validate it in the following period; thirdly, in the following period, our group will also continue to pay attention to the study of honeysuckle-forsythia pairs on the cellular level.

Acknowledgements

Not applicable.

Funding

The present study was supported by Shaanxi Provincial Department of Education 2023 Special Scientific Research Programme for Serving Localities (Industrialisation Cultivation Project) (grant no. 23JC026), Shaanxi Provincial Science and Technology Innovation Team (grant no. 2022TD-56), Special Project for Central Guided Local Science and Technology Development through a key project grant (grant no. 2019 ZY-FP-02) and the National Modern Agricultural Industrial Technology System Construction through a special project grant (grant no. CARS-21).

Availability of data and materials

The datasets used and/or analyzed during the present study are available from the corresponding author upon reasonable request.

Authors' contributions

XW and MC designed the experiments and wrote and revised the manuscript. XW, MC and WL performed the experiments and analyzed the data. MY performed the experiments. JH and MY performed the experiments. ZS and XL designed network pharmacology. RZ and YH performed the literature review. ZS, JH and XL confirm the authenticity of all the raw data. All authors have read and approved the final manuscript.

Ethics approval and consent to participate

The experimental protocols were approved by the Committee on the Ethics of Animal Experiments of Shangluo University (Shangluo, China; approval no. SLXY20210416).

Patient consent for publication

Not applicable.

Competing interests

The authors declare that they have no competing interests.

References

1. Shen Tao-Ye, Guo Jian-Hao and Wang Xiao-Juan: Research progress in the treatment of acute lung injury. Chin Mod Applied Pharm 38: 366-370, 2021.
2. Messer MP, Kellermann P, Weber SJ, Hohmann C, Denk S, Klohs B, Schultze A, Braumüller S, Huber-Lang MS and Perl M: Silencing of fas, fas associated via death domain, or caspase 3 differentially affects lung inflammation, apoptosis, and development of trauma-induced septic acute lung injury. Shock 39: 19-27, 2013.
3. Jia Xuemei and Yang Guangfu: Research progress on pathogenesis of acute lung injury/acute respiratory distress syndrome. Chin Pract Med 6: 242, 2011.
4. Yuan Wei, Yang Hui, Xie Yong, *et al*: Effect of Forsythiaside A on regulatory T cells in mice with systemic endotoxemia. Chin Patent Med 36: 1584-1588, 2014.
5. Bakowitz M, Bruns B and McCunn M: Acute lung injury and the acute respiratory distress syndrome in the injured patient. Scand J Trauma Resusc Emerg Med 20: 54, 2012.

6. Bellani G, Laffey JG, Pham T, Fan E, Brochard L, Esteban A, Gattinoni L, van Haren F, Larsson A, McAuley DF, *et al*: Epidemiology, patterns of care, and mortality for patients with acute respiratory distress syndrome in intensive care units in 50 countries. JAMA 315: 788-800, 2016.
7. Ma Xiaolong, Chen Yueru and Shen Feiyan: Research progress on therapeutic effect and mechanism of traditional Chinese medicine in acute lung injury. CJMAP 39: 269-276, 2022.
8. Xue Bingquan, Zhu Yanhui and Yu Haiyan: Study on the mechanism of Fructus Forsythiae in the treatmen to facute lung injury basedon UPLC-Q-TOF-MS/MS and network pharmacology. Chin J Hosp Pharm 42: 2208-2215, 2022.
9. Yang R, Lu Y, Hao H, Zhang MD, Xuan J and Zhang YQ: Research progress on the chemical constituents and pharmacological activities of iridoid glycosides in Lonicera japonica. Zhongguo Zhong Yao Za Zhi 46: 2746-2752, 2021 (In Chinese).
10. Xiao Xie Mengzhou and Gan Long: Determination of chlorogenic acid and total flavonoids in Lonicera japonica thunb and Lonicera japonica thunb. Chin Herb Med 50: 210-216, 2019.
11. Ji Hua, Wang Lin and Zhang Haixin: Forsythia, the Taoist traditional Chinese medicine in Hebei province. Mod Rural Sci Technol 2021: 125, 2021.
12. Gong L, Wang C, Zhou H, Ma C, Zhang Y, Peng C and Li Y: A review of pharmacological and pharmacokinetic properties of Forsythiaside A. Pharmacol Res 169: 105690, 2021.
13. Yang HX, Liu QP, Zhou YX, Chen YY, An P, Xing YZ, Zhang L, Jia M and Zhang H: Forsythiasides: A review of the pharmacological effects. Front Cardiovasc Med 9: 971491, 2022.
14. Ding Z, Zhong R, Yang Y, Xia T, Wang W, Wang Y, Xing N, Luo Y, Li S, Shang L and Shu Z: Systems pharmacology reveals the mechanism of activity of Ge-Gen-Qin-Lian decoction against LPS-induced acute lung injury: A novel strategy for exploring active components and effective mechanism of TCM formulae. Pharmacol Res 156: 104759, 2020.
15. Ding Z, Zhong R, Xia T, Yang Y, Xing N, Wang W, Wang Y, Yang B, Sun X and Shu Z: Advances in research into the mechanisms of Chinese Materia Medica against acute lung injury. Biomed Pharmacother 122: 109706, 2020.
16. Liang C, Hui N, Liu Y, Qiao G, Li J, Tian L, Ju X, Jia M, Liu H, Cao W, *et al*: Insights into forsythia honeysuckle (Lianhuaqingwen) capsules: A Chinese herbal medicine repurposed for COVID-19 pandemic. Phytomed Plus 1: 100027, 2021.
17. Zhang H, Xu L, Song J, Zhang A, Zhang X, Li Q, Qu X and Wang P: Establishment of quality evaluation method for Yinqiao powder: A herbal formula against COVID-19 in China. J Anal Methods Chem 2022: 1748324, 2022.
18. Ding X, Lin Z and Wang D: Research progress on constituents and pharmacological actions of Lonicerae Japonicae Flos, Forsythiae Fructus and their combination. Shandong science 32: 36-41, 2019.
19. Huang H: [The inheritance and development of Shang han lun (Treatise on cold pathogenic diseases) in the perspective of Wu Jutong's Wen bing tiao bian (Treatise on differentiation and treatment of seasonal warm diseases)]. Zhonghua Yi Shi Za Zhi 32: 36-38, 2002 (In Chinese).
20. Kong Yurong, Li Yan, Chen Yifan, *et al*: Analysing Wu Jutong's experience of using honeysuckle-forsythia from the theory of disposition and flavour matching. Modern Chinese Medicine Clinic 29: 52-54-67, 2022.
21. Li Y, Cai W, Weng X, Li Q, Wang Y, Chen Y, Zhang W, Yang Q, Guo Y, Zhu X and Wang H: Lonicerae Japonicae Flos and Lonicerae Flos: A systematic pharmacology review. Evid Based Complement Alternat Med 2015: 905063, 2015.
22. Chen Y, Zhang C, Wang N and Feng Y. Deciphering suppressive effects of Lianhua Qingwen Capsule on COVID-19 and synergistic effects of its major botanical drug pairs. Chin J Nat Med 21: 383-400, 2023.
23. Xu H, Huang L and Xu Y: [Simultaneous determination of five effective components in Qingrejiedu oral liquid using high performance liquid chromatography-mass spectrometry]. Se Pu 26: 599-602, 2008 (In Chinese).
24. Li R, Zhu Y, Yu M, Liu T, Zhao Y and Yu Z: Study on the mechanism of anti-acute lung injury of Shuanghuanglian oral liquid based on identification of transitional components in blood and network pharmacology. J Chromatogr B Analyt Technol Biomed Life Sci 1212: 123498, 2022.
25. Lin L: [Application of differential derivative spectrophotometry to the determination of total chlorogenic acid in Lonicera japonica Thunb. and yinqiao jiedu pian]. Zhongguo Zhong Yao Za Zhi 16: 282-284 and 318, 1991 (In Chinese).
26. Ye J, Li L and Hu Z: Exploring the molecular mechanism of action of Yinchen Wuling powder for the treatment of hyperlipidemia, using network pharmacology, molecular docking, and molecular dynamics simulation. Biomed Res Int 2021: 9965906, 2021.
27. National Research Council (US) Committee for the Update of the Guide for the Care and Use of Laboratory Animals: Guide for the Care and Use of Laboratory Animals. 8th edition. National Academies Press (US), Washington (DC), 2011.
28. Xu X, Zhang W, Huang C, Li Y, Yu H, Wang Y, Duan J and Ling Y: A novel chemometric method for the prediction of human oral bioavailability. Int J Mol Sci 13: 6964-6982, 2012.
29. Ru J, Li P, Wang J, Zhou W, Li B, Huang C, Li P, Guo Z, Tao W, Yang Y, *et al*: TCMSP: A database of systems pharmacology for drug discovery from herbal medicines. J Cheminform 6: 13, 2014.
30. Kim S, Chen J, Cheng T, Gindulyte A, He J, He S, Li Q, Shoemaker BA, Thiessen PA, Yu B, *et al*: PubChem in 2021: New data content and improved web interfaces. Nucleic Acids Res 49: D1388-D1395, 2021.
31. Chen X, Ji ZL and Chen YZ: TTD: Therapeutic target database. Nucleic Acids Res 30: 412-415, 2002.
32. Doncheva NT, Morris JH, Gorodkin J and Jensen LJ: Cytoscape StringApp: Network analysis and visualization of proteomics data. J Proteome Res 18: 623-632, 2019.
33. Tang Y, Li M, Wang J, Pan Y and Wu FX: CytoNCA: A cytoscape plugin for centrality analysis and evaluation of protein interaction networks. Biosystems 127: 67-72, 2015.
34. Huang JH Huang XH, Chen ZY, Zheng QS and Sun RY: Dose conversion among different animals and healthy volunteers in pharmacological study. Chinese Clinical Pharmacology and Therapeutics 9: 1069-1072, 2004 (In Chinese).
35. Zhou L, Yang H, Ai Y, Xie Y and Fu Y: Protective effect of Forsythiaside A on acute lung injury induced by lipopolysaccharide in mice. Xi Bao Yu Fen Zi Mian Yi Xue Za Zhi 30: 151-154, 2014 (In Chinese).
36. Arocho A, Chen B, Ladanyi M and Pan Q: Validation of the 2-deltadeltaCt calculation as an alternate method of data analysis for quantitative PCR of BCR-ABL P210 transcripts. Diagn Mol Pathol 15: 56-61, 2006.
37. Wang Z, Yu T, Hou Y, Zhou W, Ding Y and Nie H: Nie H: Mesenchymal stem cell therapy for ALI/ARDS: Therapeutic potential and challenges. Curr Pharm Des 28: 2234-2240, 2022.
38. Nova Z, Skovierova H and Calkovska A: Alveolar-Capillary membrane-related pulmonary cells as a target in endotoxin-induced acute lung injury. Int J Mol Sci 20: 831, 2019.
39. Geng Q, Liu B, Zhao PC, Xiong YB, Li L, Yi JF and Lyu C: Molecular mechanism of Fagopyri Dibotryis Rhizoma in treatment of acute lung injury based on network pharmacology and in vitro experiments. Zhongguo Zhong Yao Za Zhi 46: 4816-4823, 2021 (In Chinese).
40. Wu J, Zhang F, Li Z, Jin W and Shi Y. Integration strategy of network pharmacology in Traditional Chinese Medicine: A narrative review. J Tradit Chin Med 42: 479-486, 2022.
41. D'Alessio FR: Mouse models of acute lung injury and ARDS. Methods Mol Biol 1809: 341-350, 2018.
42. Huang CY, Deng JS, Huang WC, Jiang WP and Huang GJ: Attenuation of lipopolysaccharide-induced acute lung injury by hispolon in mice, through regulating the TLR4/PI3K/Akt/mTOR and Keap1/Nrf2/HO-1 pathways, and suppressing oxidative stress-mediated er stress-induced apoptosis and autophagy. Nutrients 12: 1742, 2020.
43. Li WW, Wang TY, Cao B, Liu B, Rong YM, Wang JJ, Wei F, Wei LQ, Chen H and Liu YX: Synergistic protection of matrine and lycopene against lipopolysaccharide-inducedacute lung injury in mice. Mol Med Rep 20: 455-462, 2019.
44. Wang J, Luo L, Zhao X, Xue X, Liao L, Deng Y, Zhou M, Peng C, Li Y: Forsythiae Fructuse extracts alleviates LPS-induced acute lung injury in mice by regulating PPAR-γ/RXR-α in lungs and colons. J Ethnopharmacol: 293:115322,2022. doi: 10.1016/j.jep.2022.115322.
45. Liu C, Xiao K and Xie L: Progress in preclinical studies of macrophage autophagy in the regulation of ALI/ARDS. Front Immunol 13: 922702, 2022.
46. Li Q, Yin J, Ran QS, Yang Q, Liu L, Zhao Z, Li YJ, Chen Y, Sun LD, Wang YJ, *et al*: [Efficacy and mechanism of Lianhua Qingwen Capsules(LHQW) on chemotaxis of macrophages in acute lung injury (ALI) animal model]. Zhongguo Zhong Yao Za Zhi 44: 2317-2323, 2019 (In Chinese).

47. Wang Y, Yuan Y, Wang W, He Y, Zhong H, Zhou X, Chen Y, Cai XJ and Liu LQ: Mechanisms underlying the therapeutic effects of Qingfeiyin in treating acute lung injury based on GEO datasets, network pharmacology and molecular docking. Comput Biol Med 145: 105454, 2022.
48. Liu Jiao and Li Mingchun: The relationship between PI3K/ATK pathway and EGFR tyrosine-kinase inhibitor resistance. Chinese Journal of Pharmacology 29: 1648-1650, 2013.
49. Liu B, Yu H, Baiyun R, Lu J, Li S, Bing Q, Zhang X and Zhang Z: Protective effects of dietary luteolin against mercuric chloride-induced lung injury in mice: Involvement of AKT/Nrf2 and NF-κB pathways. Food Chem Toxicol 113: 296-302, 2018.
50. Zhan Q, Ma X and He Z. PEAR1 suppresses the proliferation of pulmonary microvascular endothelial cells via PI3K/AKT pathway in ALI model. Microvasc Res 128: 103941, 2020.
51. Lai WY, Wang JW, Huang BT, Lin EP and Yang PC: A novel TNF-α-targeting aptamer for TNF-α-mediated acute lung injury and acute liver failure. Theranostics 9: 1741-1751, 2019.
52. Yang Z, Zhang XR, Zhao Q, Wang SL, Xiong LL, Zhang P, Yuan B, Zhang ZB, Fan SY, Wang TH and Zhang YH: Knockdown of TNF-α alleviates acute lung injury in rats with intestinal ischemia and reperfusion injury by upregulating IL-10 expression. Int J Mol Med 42: 926-934, 2018.
53. Peng LY, Yuan M, Song K, Yu JL, Li JH, Huang JN, Yi PF, Fu BD and Shen HQ: Baicalin alleviated APEC-induced acute lung injury in chicken by inhibiting NF-κB pathway activation. Int Immunopharmacol 72: 467-472, 2019.
54. Millar MW, Fazal F and Rahman A: Therapeutic targeting of NF-κB in acute lung injury: A double-edged sword. Cells 11: 3317, 2022.
55. Zhang JB, Jin HL, Feng XY, Feng SL, Zhu WT, Nan HM and Yuan ZW: The combination of *Lonicerae Japonicae Flos* and *Forsythiae Fructus* herb-pair alleviated inflammation in liver fibrosis. Front Pharmacol 13: 984611, 2022.
56. Shen F, Zou LS, Wen HM, Cui XB, Yu S, Zhu HX, Li C, Tian G and Shao JG: Qualitative evaluation of Forsythia suspensa by HPLC-PDA fingerprint combined with UFLC-QTOF-MS qualitative identification. Zhongguo Zhong Yao Za Zhi 44: 4495-4603, 2019 (In Chinese).
57. Landelle C, Nocquet Boyer V, Abbas M, Genevois E, Abidi N, Naimo S, Raulais R, Bouchoud L, Boroli F, Terrisse H, *et al*: Impact of a multifaceted prevention program on ventilator-associated pneumonia including selective oropharyngeal decontamination. Intensive Care Med 44: 1777-1786, 2018.
58. Yang B, Meng QY, Chen H, Gao YL, Shen J, Mu YY and Xia YB: Clinical effect of acupuncture combined with traditional Chinese medicine in treatment of oligozoospermia/asthenozoospermia: A meta-analysis. Zhen Ci Yan Jiu 45: 243-250, 2020 (In Chinese).
59. Gaweł S, Wardas M, Niedworok E and Wardas P: Malondialdehyde (MDA) as a lipid peroxidation marker. Wiad Lek 57: 453-455, 2004 (In Polish).
60. Miao L and St Clair DK: Regulation of superoxide dismutase genes: Implications in disease. Free Radic Biol Med 47: 344-356, 2009.
61. Yang L, Bi L, Jin L, Wang Y, Li Y, Li Z, He W, Cui H, Miao J and Wang L: Geniposide ameliorates liver fibrosis through reducing oxidative stress and inflammatory respose, inhibiting apoptosis and modulating overall metabolism. Front Pharmacol 12: 772635, 2021
62. Xu W, Wang M, Cui G, Li L, Jiao D, Yao B, Xu K, Chen Y, Long M, Yang S and He J: Astaxanthin protects OTA-Induced lung injury in mice through the Nrf2/NF-κB pathway. Toxins (BaseL) 11: 540, 2019.
63. Zhu S, Wei X, Yang X, Huang Z, Chang Z, Xie F, Yang Q, Ding C, Xiang W, Yang H, *et al*. Plasma lipoprotein-associated phospholipase A2 and superoxide dismutase are independent predicators of cognitive impairment in cerebral small vessel disease patients: Diagnosis and assessment. Aging Dis 10: 834-846, 2019.
64. Mauad T, Duarte-Neto AN, da Silva LFF, de Oliveira EP, de Brito JM, do Nascimento ECT, de Almeida Monteiro RA, Ferreira JC, de Carvalho CRR, do Nascimento Saldiva PH and Dolhnikoff M: Tracking the time course of pathological patterns of lung injury in severe COVID-19. Respir Res 22: 32, 2021.
65. Tang J, Xu L, Zeng Y, Gong F: Effect of gut microbiota on LPS-induced acute lung injury by regulating the TLR4/NF-kB signaling pathway. Int Immunopharmacol: 91:107272,2021. doi: 10.1016/j.intimp.2020.107272.